Micelle-like Nanoassemblies of Short Peptides Create Antimicrobial Selectivity in a Conventional Antifungal Drug

Morita, Kenta

Nishimura, Yuya

Ishii, Jun

Maruyama, Tatsuo

(Citation)
ACS Applied Nano Materials,6(2):1432-1440

(Issue Date)
2023-01-27

(Resource Type)
journal article

(Version)
Accepted Manuscript

Micelle-Like Nano-Assembly of Short Peptide Creates Antimicrobial Selectivity in a Conventional Antifungal Drug

Kenta Morita[†], Yuya Nishimura[‡], Jun Ishii[‡], and Tatsuo Maruyama[*†]*

[†]PhD K. Morita, Prof. PhD. T. Maruyama*

Department of Chemical Science and Engineering, Graduate School of Engineering

Kobe University

1-1 Rokkodai, Nada-ku, Kobe 657-8501, Japan.

E-mail: tmarutcm@crystal.kobe-u.ac.jp

[‡]PhD Y. Nishimura, Prof. PhD J. Ishii

Division of Biotechnology and Environmental Technology, Graduate School of Science, Technology and Innovation

Kobe University

1-1 Rokkodai, Nada-ku, Kobe 657-8501, Japan.

Abstract: The discovery of novel antibacterial drugs against infectious diseases has decreased over the last few decades because of their poor cost performance. In this study, we report that the nano-assembly of a short-peptide hydrogelator (P1) endowed novel antifungal selectivity to a conventional antifungal drug, amphotericin B (AmB), which expands its application spectrum. Clinical use of AmB is limited because of poor water solubility and poor selectivity in its toxicity, which often causes harmful effects on tissues. P1 was the low-molecular weight hydrogelator (LMWHg) that showed low cytotoxicity and was enzymatically degraded. In general, an LMWHg entraps foreign hydrophobic molecules inside the hydrophobic space in the self-assembled body. P1 successfully solubilized AmB in water as a form of a nanocomplex (NC) that had a chain-like structure. The NCs showed remarkably low toxicity toward *Saccharomyces cerevisiae* as a model fungus when compared with free AmB, meaning that P1 suppressed the antifungal activity of AmB via co-assembly. The suppressed antifungal activity of AmB recovered when P1 in the NCs was degraded by a protease to liberate AmB from the co-assembly with P1. P1 at a high concentration formed a hydrogel incorporating AmB (AmB-P1 gel), in which the antifungal activity of AmB was suppressed as well as that in the NC. The co-assembly with AmB affected the morphology of the P1 self-assembly. While *S. cerevisiae* that did not secrete proteases formed a colony on the AmB-P1 gel, *Aspergillus oryzae* that secreted proteases did not grow on the AmB-P1 gel at all, resulting in the selective killing of the fungus. Because some of malignant, infectious fungi secrete proteases, the co-assembly strategy of conventional antifungal drugs with self-assembling molecules should lead to “drug repositioning” of approved drugs in the health and medical fields.

KEYWORDS: Antifungal drug, drug repositioning, low-molecular-weight gelator, peptide, self-assembly

1. INTRODUCTION

Since the discovery of penicillin in 1928, antimicrobial drugs have saved many humans from infectious diseases.[1–3] Although antimicrobial drugs have contributed enormously to human health, the discovery of novel antimicrobial agents has decreased.[4,5] Pharmaceutical companies have withdrawn from developing new antimicrobials because of the repeated emergence of drug-resistant bacteria and the limited duration of approved treatment, leading to a low profit-to-development cost ratio. Therefore, there is an emerging trend that conventional drugs approved for a specific disease are used to treat other diseases, requiring no regulatory approval.[6] This concept is called "drug repositioning,"[7,8] which has been used to treat coronavirus infections.[9]

Amphotericin B (AmB) is a conventional antifungal drug belonging to the macrolide class. AmB was approved 50 years ago and is still in active medical use because of its broad antifungal spectrum and no emergence of resistant bacteria in clinical practice.[10–12] However, AmB has two drawbacks. First, AmB is barely soluble in water. A dispersant such as deoxycholic acid or liposomes is currently required to formulate AmB. Second, AmB has non-specific toxicity toward fungi and normal tissues.[13,14] AmB binds preferably to ergosterol, which exists only in cell membranes of fungi, and forms a channel in the cell membrane to disrupt the ion balance of fungus cells.[15,16] AmB exhibits a weak affinity to cholesterol in mammalian cell membranes,[17] which results in side effects in the tissues of treated patients. Additionally, treatment with AmB poses a potential health risk because this drug may completely eradicate indigenous fungi in patients because of a lack of specificity toward fungal species.

Infectious fungi, such as *Aspergillus*,[18] *Candida,*[19] *Cryptococcus,*[20] and *Trichophyton*[21] were reported to infect host tissues by secreting proteases.[22,23] Strains that secrete large amounts of

proteases were found in infected tissues of malignant, infectious cases.[24] Thus, developing antifungal drugs specific to strains that secrete proteases is of great significance.

A low-molecular-weight hydrogelator (LMWHg) gelates water by self-assembly.[25–28] The gelator molecules self-assemble via non-covalent bonds (e.g., hydrogen bond, electrostatic interaction, coordination, dispersion force) to form a three-dimensional fibrous structure. We previously reported several short-peptide-type LMWHg for a medical application.[29–31] Among them, acetyl-Phe-Phe-Phe-Gly-Lys (P1) was obtained as a novel LMWHg. P1 can gelate an aqueous solution in a low concentration. P1 showed low toxicity to mammalian cells and microorganisms and was enzymatically degraded,[32] while a peptide with the similar sequence to P1 was reported as an antimicrobial peptide.[33] In general, an LMWHg entraps foreign hydrophobic molecules inside the hydrophobic space in the self-assembled body, which can be used for a drug delivery system.[34–37] We hypothesized that AmB can also be entrapped (co-assembled) in micelles or the fibrous structures of P1 (Fig. 1).

In this study, we aimed to "drug reposition" AmB using an LMWHg via their co-assembly. The co-assembly formation created the antimicrobial selectivity in AmB, which would expand its application in the medical and sanitary fields. The present strategy is as follows: (1) to suppress the non-specific toxicity of AmB via co-assembly with P1; and (2) to recover the antifungal activity of AmB by release from the co-assembly in the presence of a protease secreted by infectious fungi. This strategy is the first trial to re-use a conventional drug already marketed by combining it with an LMWHg.

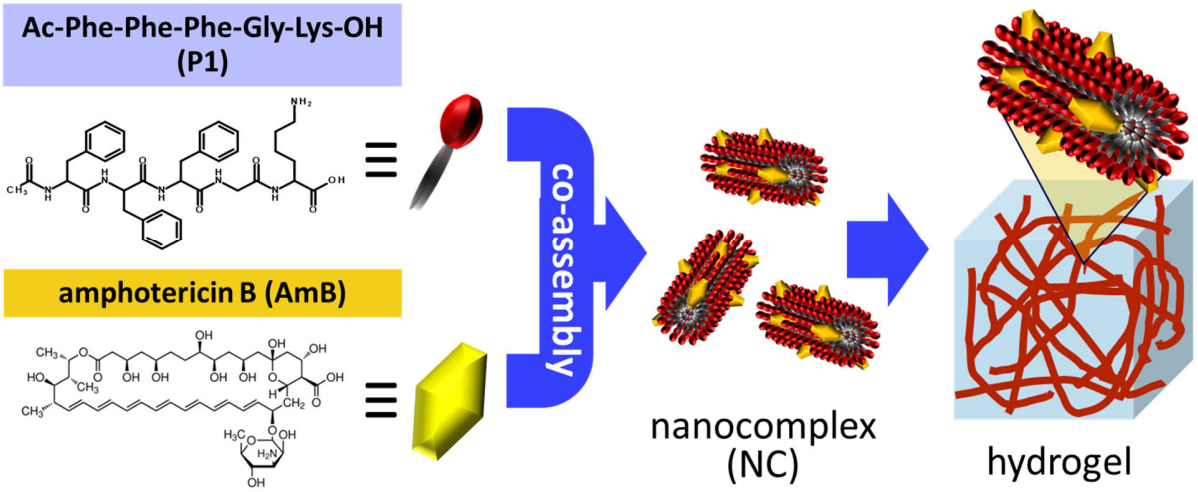

Figure 1. Schematic illustration of the co-assembly of an amphiphilic short-peptide hydrogelator (P1) and amphotericin B to produce a nanocomplex and a hydrogel.

2. EXPERIMENTAL SECTION

2.1. Materials

Fmoc-amino acids, amino acid pre-loaded resins, 2-(1H-benzotriazole-1-yl)-1,1,3,3-tetramethyluronium hexafluorophosphate (HBTU), 1-hydroxybenzotriazole·H_2O (HOBT·H_2O), triisopropylsilane (TIPS) and *N,N*-dimethylformamide (DMF) were purchased from Watanabe Chemical Industry (Hiroshima, Japan). Trifluoroacetic acid (TFA), dichloromethane (DCM), methanol, diethyl ether, acetonitrile, magnesium sulfate heptahydrate ($MgSO_4·7H_2O$), potassium dihydrogen phosphate (KH_2PO_4), dimethyl sulfoxide (DMSO) and 12 tungsto (VI) phosphoric acid n-hydrate were purchased from FUJIFILM Wako Pure Chemical Corporation (Osaka, Japan). Piperidine, *N,N*-diisopropylethylamine (DIEA), and 2,5-dihydroxybenzoic acid (DHB) were purchased from Tokyo Chemical Industry (Tokyo, Japan). Dulbecco's phosphate-buffered saline (PBS), yeast extract, tryptone, kanamycin, skim milk, purified agar, D-glucose, and alpha-

chymotrypsin was purchased from Nacalai Tesque (Kyoto, Japan). A phosphorylated peptide amphiphile was purchased from Cosmo Bio (Tokyo, Japan). Amphotericin B (AmB) was purchased from Chem-Impex International (Wood Dale, IL, USA). Tween 20 was purchased from Calbiochem (La Jolla, CA, USA). Potato Dextrose Agar "Nissui" was purchased from Nissui Pharmaceutical (Tokyo, Japan). Bacto peptone was purchased from Becton, Dickinson and Company (Franklin Lakes, NJ, USA).

2.2. Solid-phase synthesis of peptides

Peptides were synthesized on Fmoc-Lys(Boc)-Alko resin using the standard Fmoc solid-phase peptide synthesis method. A Fmoc-protected amino acid (3 equivalents) was coupled to 0.3 mmol amino-acid-pre-loaded Alko resin using HBTU and HOBT as the coupling agents in the presence of DIEA in DMF. The crude peptides were cleaved manually from the solid support, and the side chains were deprotected using a TFA/TIPS/water (95:2.5:2.5 in volume) mixture at room temperature for 2 h. The crude peptides were precipitated and washed three times in diethyl ether and centrifuged at 10000 × *g* for 5 min. The precipitates were lyophilized overnight. A high-performance liquid chromatography (HPLC) system, Shimadzu LC-20AT, equipped with a UV-vis detector SPD-20A was used to purify all crude peptides. The settings were: eluent A, 0.1% TFA in water; eluent B, 0.1% TFA in acetonitrile; gradient, 0–100% eluent B over 20 min; detection wavelength, 230 nm. The final compound was characterized by matrix-assisted laser desorption ionization-time of flight mass spectrometer (MALDI-TOF/MS) measurements using an UltrafleXtreme mass spectrometer (Bruker, Billerica, MA, USA). The purified peptides were obtained after lyophilization of the collected HPLC fractions. The obtained peptides were stored at –16 °C until use.

2.3. Preparation of nanocomplexes of AmB and P1 (AmB-NCs)

Unless otherwise stated, 0.2 mg mL^{-1} AmB and 0.2% P1 were added to 10 mM phosphate buffer (pH 6.8). The solution was heated on a hot stirrer at 100 °C for 5 min with stirring, followed by cooling at room temperature for 2 h. The supernatant was centrifuged at 1600 × *g* for 15 min to remove undissolved AmB, and the supernatant was obtained as a dispersion of AmB-NCs. AmB-NCs were used for experiments on the same day of preparation. AmB in the dispersion of AmB-NCs was quantified using HPLC with the same settings as those for the peptide purification, except the detection wavelength was 405 nm.

2.4. Dynamic light scattering (DLS) analysis

Diameter distributions of the P1 nano-assembly and AmB-NCs were measured using a ELSZ1000 (Otsuka Electronics, Osaka, Japan). Measurements were performed using 1 mL sample solution in a plastic disposable cell.

2.5. Confirmation of co-assembly of AmB and P1

A dispersion of AmB-NCs and a saturated AmB solution were passed through a DISMIC cellulose acetate membrane filter (Advantec, Tokyo, Japan) with a pore size of 0.20, 0.45, or 0.80 μm. The AmB in the filtrate was quantified using HPLC.

2.6. Effect of Tween 20 on the solubility of AmB

AmB was added to 10 mM phosphate buffer containing Tween 20 to give a final AmB concentration of 0.2 mg mL^{-1}. The solution was heated on a hot stirrer at 100 °C for 5 min with

stirring, followed by cooling at room temperature for 2 h. The supernatant was centrifuged at 1600 × *g* for 15 min to remove undissolved AmB. The concentration of AmB was determined by HPLC.

2.7. Strains

Aspergillus oryzae RIB40 (*A. oryzae*), *Saccharomyces cerevisiae* BY4741 (*S. cerevisiae*), and *Escherichia coli* MG1655 (*E. coli*) were used.

2.8. Growth media

Yeast extract/peptone/dextrose (YPD) medium: 1% yeast extract, 2% peptone, and 2% D-glucose

Lysogeny broth (LB) medium: 0.5% yeast extract, 1% tryptone, and 1% NaCl

Yeast extract/peptone/dextrose/agar (YPDA) medium: 1% yeast extract, 2% peptone, and 2% D-glucose, and 1.5 % agarose

Lysogeny broth/agar (LBA) medium: 0.5% yeast extract, 1% tryptone, and 1% NaCl, and 1.5 % agarose

Potato/dextrose/agar (PDA) medium: 3.9% Potato Dextrose Agar "Nissui"

Czapek-Dox medium modified for high protease-secretion by A. oryzae (MCD medium)[38]: 1% KCl, 2% KH_2PO_4, 2% $MgSO_4 \cdot 7H_2O$, 0.002% $FeSO_4 \cdot 7H_2O$, 3.6% D-glucose, and 3% skim milk

YPD medium and LB medium were sterilized by autoclaving. YPDA, LBA, and PDA media were solidified into plates after autoclaving. *S. cerevisiae*, *E. coli*, and *A. oryzae* were maintained on YPDA, LBA, and PDA plates, respectively. The MCD medium was autoclaved without skim milk and completed by adding skim milk just before use.

2.9. Preparation of gels containing AmB

P1 and AmB were added to 10 mM phosphate buffer (pH 6.8) at 1.0 wt% and 200 μg mL^{-1}, respectively, and heated on a hot stirrer at 100 °C for 5 min with stirring. The hot solution was gelated by cooling at room temperature for at least 3 h (AmB-P1 gel). "P1 gel" was prepared from P1 without AmB using the same procedure. YPD medium and MCD medium were gelated using the same procedure as the AmB-P1 gel to prepare "AmB-P1/YPD solid medium" and "AmB-P1/MCD solid medium", respectively.

AmB was dissolved in DMSO at 20 mg mL^{-1}. The AmB-DMSO solution (10 μL) was added to 10 mM phosphate buffer (pH 6.8) (1 mL) containing 1.5 wt% agarose (AmB-agar gel). YPD medium and MCD medium were gelated using the same procedure as the AmB-agar gel to prepare "AmB-agar/YPD solid medium" and "AmB-agar/MCD solid medium".

These gels were used for the antifungal activity assay after storage overnight at 4 °C.

2.10. Microscopic observation

2.10.1. Transmission electron microscope (TEM) observation

A P1 nano-assembly, AmB-NCs, P1 gel, and AmB-P1 gel were prepared as described above. A cupper grid supported by an elastic carbon film (ELW-C10; STEM, Tokyo, Japan) was modified to be hydrophilic using an ion cleaner (JEOL, Tokyo, Japan). A sample solution was mounted on the grid, followed by a negative staining using 2 wt% 12 tungsto (VI) phosphoric acid aqueous solution. A TEM observation was conducted using a JEM-2100F instrument (JEOL, Tokyo, Japan).

2.10.2. Scanning probe microscope (SPM) observation

An AmB-P1 gel, which was heated at 100 °C, was placed on a cover glass and vacuumed dried in a desiccator for three days at room temperature. A sample was observed in the dynamic force

microscope mode using a SPA-400/NanoNavi II equipped with an SI-DF20 cantilever (Hitachi High-Tech, Tokyo, Japan) in 512×512 pixels.

2.11. Rheology measurement

Rheology measurements were performed using an MCR301 (Anton Paar Physica, Graz, Austria) with a parallel plate with 25-mm diameter. For the sample preparation, P1 gel and AmB-P1 gel were prepared at room temperature on a 21-mm diameter glass dish. The gel disc was placed on the stage and a frequency sweep measurement was carried out at a strain of 0.1 % and a gap of 2.0 mm.

2.12. Pre-culture conditions

S. cerevisiae was inoculated into 5 mL YPD medium in a glass tube and cultured for 16 h at 30 °C with rotary shaking (150 rpm). *E. coli* was inoculated into 5 mL LB medium in a glass tube and cultured for 16 h at 37 °C with reciprocal shaking (200 rpm). *A. oryzae* was inoculated on a PDA plate and cultured for two weeks at 30 °C. A recovery solution for conidia of *A. oryzae* was prepared by dissolving 0.1 wt% Tween 80 and 0.8% NaCl in water. The conidia were collected using a scraper after adding 10 mL recovery solution.

2.13. Antifungal activity assay of nanocomplexes

Nanocomplexes were diluted with a culture medium to give varied drug concentrations, and 95 μL samples were pipetted into wells of a 96-well plate. Pre-cultured *S. cerevisiae* was diluted with medium to an OD_{660} = 0.01 and inoculated into a well with 5 μL. The OD_{660} was measured using a multi-plate reader (SH9000, Hitachi High-Technologies Corporation, Tokyo, Japan) after

incubation at 30 °C for 24 h statically. The cells were dispersed thoroughly by hand-shaking before measurements. A fungal viability was calculated using the following equation.

$$\%\, Viability = \frac{D_s - D_{s0}}{D_c - D_{c0}} \times 100$$

, where D_{s0} and D_s were OD660 of fungus culturing media with drug samples 0 h and 24 h after incubation, respectively. D_{c0} and D_c are OD660 of fungus culturing media without drug samples 0 h and 24 h after incubation, respectively. A fifty percent inhibition concentration (IC_{50}) was calculated by interpolation linearly from the dose-growth curve.

2.14. Antibacterial activity assay of kanamycin (KM)

KM and P1 were dissolved in 10 mM phosphate buffer (pH 6.8) at 100 μg mL^{-1} and 0.2 wt%, respectively, by heating at 100 °C for 5 min. The solution was diluted with an LB medium, and 95 μL samples were pipetted into wells of a 96-well plate. The concentration of *E. coli* was measured as OD_{660}.[39,40] Pre-cultured *E. coli* was diluted with medium to an OD_{660} = 0.001 and 5 μL of this dilution was inoculated into a well. The OD_{660} was measured using the multi-plate reader after incubation at 37 °C for 24 h statically.

2.15. Antifungal activity assay of solid media containing AmB

Three hundred microliters of AmB-P1/YPD solid medium and AmB-agar/YPD solid medium were prepared in wells of a 24-well plate. Pre-cultured *S. cerevisiae* was diluted to an OD_{660} = 1 × 10^{-5} and 20 μL of this dilution plated onto the solid media. Colony formation was observed after incubation for three days at 30 °C.

2.16. Inhibition of free AmB by P1 nano-assembly without heating

AmB was dissolved in DMSO at 20 mg mL^{-1} as a stock solution of free AmB (AmB/DMSO). An AmB/DMSO solution was added to 3 mL YPD medium at 1 μg mL^{-1} in an L-type culture tube (TV100030; Advantec). Pre-cultured *S. cerevisiae* was inoculated into the medium to give an OD_{660} = 0.1, followed by the addition of the P1 solution. Cell growth was monitored using a rocking incubator equipped with a spectrophotometer (TVS062CA; Advantec). The OD_{660} was recorded every 10 min using the TVS062CA according to culturing at 30 °C with a rocking shake at 40 rpm. Data were averaged from duplicate experiments.

2.17. Recovery of antifungal activity of AmB using ChT

ChT was dissolved in 20 mM HCl at 200 μg mL^{-1} to give the stock solution. AmB-NCs and ChT were added separately into 3 mL YPD medium at 1 μg mL^{-1} and 0.33 μg mL^{-1}, respectively. Pre-cultured *S. cerevisiae* was inoculated into the medium to give an OD_{660} = 0.1. Cell growth (OD_{660}) was recorded every 10 min according to culturing at 30 °C with a rocking shake at 40 rpm using the TVS062CA. Data were averaged from duplicate experiments.

2.18. Release of AmB from hydrogels

A ChT stock solution (100 μL) was diluted by 10 mM phosphate buffer (900 μL) and its pH was adjusted to 7.5 using 3% Na_2CO_3 aqueous solution. An AmB-P1 gel and an AmB-agar gel were prepared in glass vials in 1 mL each. The hydrogels were incubated at 37 °C after addition of the ChT solution or phosphate buffer. Aliquots (100 μL) were periodically taken from the liquid phase and analyzed by HPLC.

2.19. Detection of proteases secreted by fungi

Three hundred microliters of MCD (or YPD) media gelated with 1 wt% P1 or 1.5 wt% agarose were prepared in a 24-well plate. Pre-cultured *S. cerevisiae* was diluted to an $OD_{660} = 1 \times 10^{-5}$ and 20 μL inoculated onto the two different media. *A. oryzae* was inoculated with 100 conidia onto the media. After incubating for five days at 30 °C, the secreted proteases were recovered by adding 1 mL PBS to the culture medium with gentle pipetting. The liquid was centrifuged at 3800 × *g* to eliminate solid residues, and the proteases in the supernatant were detected using the Amplite Universal Fluorimetric Protease Activity Assay Kit Green (AAT Bioquest, Sunnyvale, CA, USA). The enzyme unit (U) was defined as the amount of the enzyme that catalyzes the conversion of one micromole of the substrate per minute.

2.20. Degradation of P1 by proteases secreted by fungi

A. oryzae was cultured on MCD solid medium gelated by 1.5 wt% agarose in a 24-well plate for 5 days. P1 was dissolved in PBS at 0.1 wt%. The P1 solution (200 μL) was added on the cell culturing medium. After incubation at 30 °C for 2 h, the supernatant (10 μL) was applied to a MALDI-TOF/MS analysis.

2.21. Selective killing of a fungus secreting proteases

AmB-P1/MCD solid medium and AmB-agar/MCD solid medium (100 μL each) were prepared in a 96-well plate. Ten microliters of pre-cultured *S. cerevisiae* at an $OD_{660} = 0.01$ and 100 conidia of *A. oryzae* were inoculated onto the media. Colony formation was observed using a microscope after incubation for 48 h at 30 °C. As controls, AmB-agar/YPD solid medium and AmB-P1/YPD solid medium were prepared using the same procedure as the MCD solid medium, which were used for culturing *A. oryzae*.

2.22. Statistical analysis

Results are presented as mean ± standard deviation. Data were analyzed statistically by Student's t-test. All data were analyzed using Microsoft Excel 2016 (16.0.4266.1001). Statistical significance was set at $*p < 0.05$, $**p < 0.01$.

3. RESULTS AND DISCUSSION

P1 was prepared using Fmoc solid-phase synthesis and confirmed by MALDI-TOF/MS (Fig. S1). P1 was dissolved in 10 mM phosphate buffer (pH 6.8) at 0.2 wt% with heating. Subsequent cooling at room temperature yielded a P1 nano-assembly dispersion. The dynamic light scattering (DLS) analysis indicated that the diameter of the P1 nano-assembly ranged in 300-1000 nm (Fig. 2a). TEM observation revealed a polymorph of the P1 nano-assembly, which contained spherical nanoparticles of 30-50 nm and short fibers (Fig. 2b(i)). Some of the nanoparticles were aggregated at several hundred nanometers in length, which agreed with the DLS measurements. We then investigated the co-assembly of P1 and AmB. P1 (0.2 wt%) and AmB (0.2 mg mL^{-1}) were dissolved in phosphate buffer upon heating. The resultant dispersion was termed a nanocomplex consisting of AmB and P1 (AmB-NCs). The existence of the AmB-NCs was demonstrated by Tyndall scattering, and their diameters ranged from 100 to 300 nm (Fig. 2a). TEM observation revealed that the AmB-NC had a chain-like structure. Nanoparticles less than 30 nm in diameter were continuously connected (Fig. 2b(ii)). Fibers were not found in the AmB-NCs dispersion. AmB would disturb the formation of a fiber by co-assembling with P1, leading to a decrease of the diameter comparing to that of P1 nano-assembly.

The co-assembly of AmB and P1 in the AmB-NCs was confirmed using membrane filtration. When a dispersion of the AmB-NCs was passed through a membrane filter, the AmB concentration in the filtrate was much lower than that of the AmB-saturated solution (Fig. 2c). Membrane filters with pore sizes of 0.2 and 0.45 μm gave only less than 5% of the applied AmB to the filtrates, showing that the major portion of AmB in the AmB-NCs was rejected by the membranes. A membrane filter with a pore size of 0.8 μm also rejected approx. 78% AmB in a dispersion. The membrane filtration of an AmB-saturated solution (free AmB) resulted in AmB concentrations much higher than those for the AmB-NCs. These results indicated that a large portion of AmB-NCs were more than 0.45 μm in diameter and that free AmB in a saturated solution passed through the membrane filters. These results also suggest that AmB and P1 co-assembled to form AmB-NCs.

The solubility of AmB is only 2.0 μg mL^{-1} in phosphate buffer. The co-assembly with P1 should solubilize AmB in the buffer. We quantified the solubilized AmB in the presence of P1. The concentration of the solubilized AmB increased as the P1 concentration increased (Fig. 2d). These investigations were conducted below the minimum gelation concentration (MGC) of P1. These results also support the co-assembly of AmB with P1. We also employed Tween 20 as a surfactant to prepare micelles co-assembled with AmB in phosphate buffer. Interestingly, Tween 20 (1 wt%) did not increase the solubility of AmB in phosphate buffer.

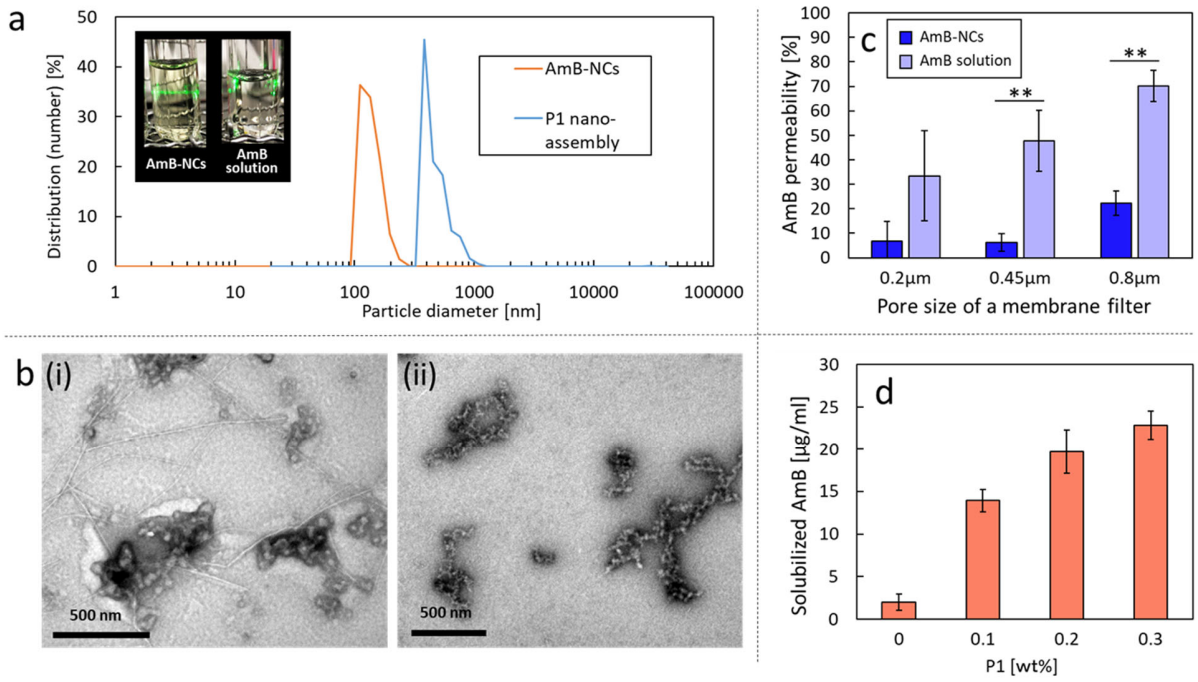

Figure 2. (a) Size distribution of the P1 nano-assembly and the AmB-NCs prepared with 0.2 mg mL^{-1} AmB and 0.2 wt% P1 measured by the dynamic light scattering analysis. Inset image represents Tyndall scattering of the AmB-NCs. (b) Transmission electron microscope images of (i) the P1 nano-assembly and (ii) the AmB-NCs. (c) AmB concentrations in the filtrates of the AmB-NCs using membrane filtration. (d) AmB concentrations solubilized in phosphate buffer via co-assembly with P1.

P1 produces a hydrogel (P1 gel) above the concentration of its MGC (Fig. 3a(i)). The effect of the co-assembly formation of AmB and P1 on the MGC was investigated (Table S1). P1 gelated 10 mM phosphate buffer above 0.4 wt% within 1 h. When 0.2 mg mL^{-1} AmB was added to a P1 solution, the MGC increased to 0.8 wt%. Then, we prepared a hydrogel with 1.0 wt% P1 and 200 μg mL^{-1} AmB (AmB-P1 gel). The obtained hydrogel was yellowish and transparent (Fig. 3a(ii)). The morphology of the P1 assembly and the AmB-P1 co-assembly in the hydrogel was observed

using a scanning probe microscope. Figure 3b(i) and (ii) show nanofibers derived from P1 (and AmB) fibrous assembly. More magnified images were provided in Figure S2. The nanofibers composed of AmB and P1 were shorter and thinner than those of P1 only. These observations also suggested that AmB disturbed the formation of the well-ordered molecular assembly and of the bundled broad fiber, although AmB did not completely inhibit a gel formation.

TEM observations were conducted to examine the effect of the co-assembly in detail. Fibers of the P1 gel were straight and uniformly 10-nm in width (Fig. 3c(i)). Fibers of the AmB-P1 gel had the same width as those of the P1 gel, but they were relatively short and branched (Fig. 3c(ii)). The fibers of the AmB-P1 gel seemed to be terminated with nano-sized spherical structures. The nano-sized spherical structure was similar to that in the AmB-NCs (Fig. 2b(ii)).

Rheological properties of the P1 gel and the AmB-P1 gel were examined using a rheometer. The storage modulus (G') and loss modulus (G'') were measured in frequency sweep experiments at a fixed strain of 0.1% (Fig. S3). G' was higher than G'' in both hydrogels, indicative of gel. Both G' and G'' of the AmB-P1 gel were lower than those of the P1 gel. The low moduli of the AmB-P1 gel would be due to in the co-assembly of AmB and P1.

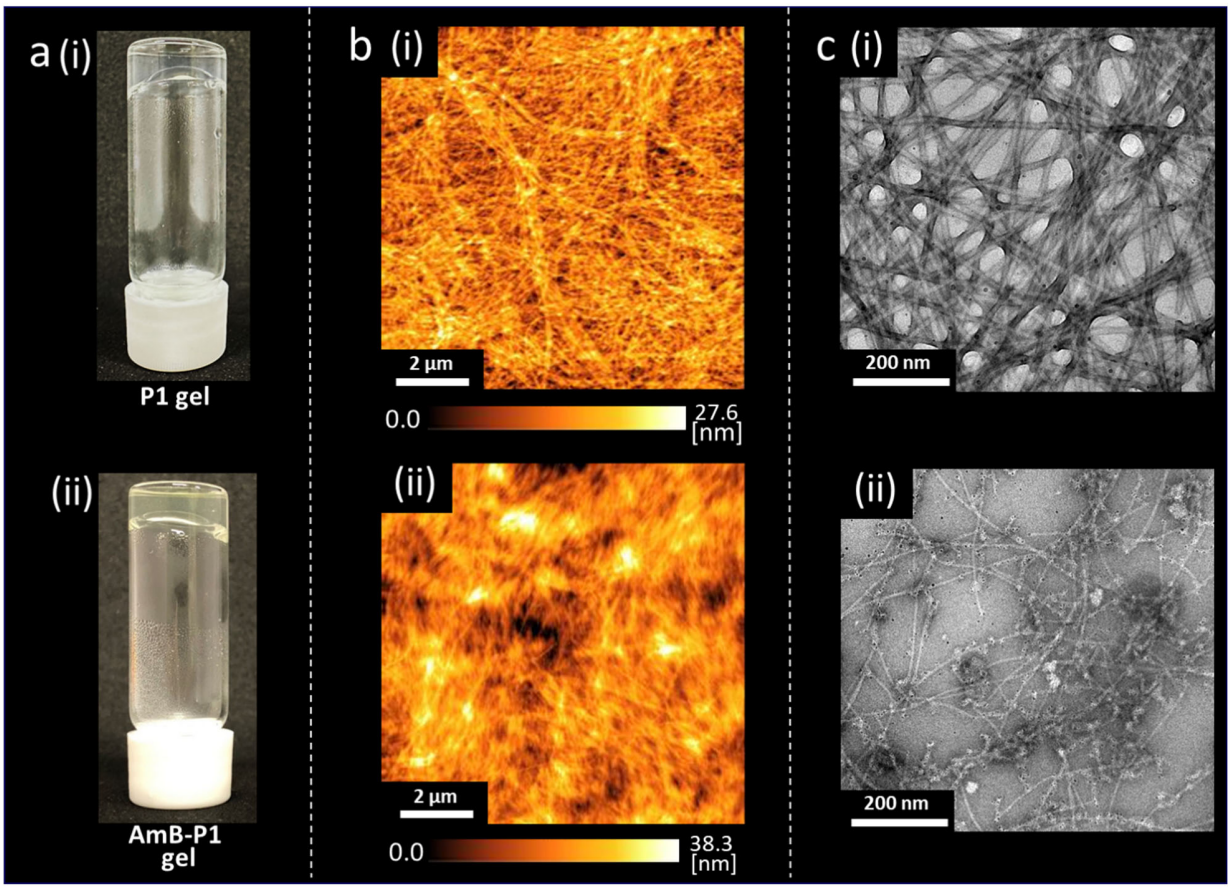

Figure 3. (a) Appearance of (i) a hydrogel prepared with only 1.0 wt% P1 and (ii) a hydrogel with 1.0 wt% P1 and 200 µg mL^{-1} AmB (AmB-P1 gel). (b) Scanning probe microscope images and (c) transmission electron microscope images of hydrogels. (i) a hydrogel prepared with only P1 and (ii) a hydrogel with P1 and AmB.

The effect of the co-assembly on the antimicrobial activity of drugs was investigated. AmB was used as a hydrophobic drug, and kanamycin (KM) was as a hydrophilic drug. The antimicrobial activity was assayed using *Saccharomyces cerevisiae* and *Escherichia coli* as models of a fungus and bacterium, respectively. *S. cerevisiae* was cultured in a liquid YPD medium with additives for one day. Free AmB showed remarkable antifungal activity at low concentrations (Fig. 4a). The AmB-NCs showed minimal antifungal activity toward *S. cerevisiae*. The antibacterial activity of

KM dissolved in LB medium with P1 was not significantly different from that of a free KM solution (Fig. S4). Consequently, P1 was able to suppress the antimicrobial activity of only AmB.

The suppression of the antifungal activity of AmB is attributed to the co-assembly of AmB and P1 and the strong interaction between them. Inhibition of AmB was also observed when free AmB was added to a P1 nano-assembly dispersion without heating (Fig. S5). The results indicated that the P1 nano-assembly formed interactions with AmB to suppress the antifungal activity. The suppression efficiency observed here was lower than that of the AmB-NCs. This would be explained as follows. When free AmB was added to a P1 nano-assembly dispersion without heating, AmB was supposed to be adsorbed to the surface of the P1 nano-assembly, not encapsulated in the nano-assembly. The adsorption equilibrium would result in the low suppression efficiency.

As described above, the co-assembly of P1 and AmB produced a hydrogel above the MGC of P1. The antifungal activity of AmB was also tested on a gelated medium using *S. cerevisiae.* We prepared a 1.5 wt% agar hydrogel containing YPD and AmB (AmB-agar YPD gel) and a 1 wt% P1 hydrogel containing YPD and AmB (AmB-P1 YPD gel). After three days of incubation, the growth of *S. cerevisiae* was inhibited completely on the AmB-agar YPD gel with AmB concentrations above 10 μg mL^{-1} (Fig. 4b(i)). In contrast, the growth of *S. cerevisiae* was not inhibited fully on the AmB-P1 YPD gel at all AmB concentrations tested (Fig. 4b(ii)). The P1 hydrogel suppressed the antifungal activity of AmB via co-assembly, which is consistent with that of the AmB-NCs in a liquid YPD medium.

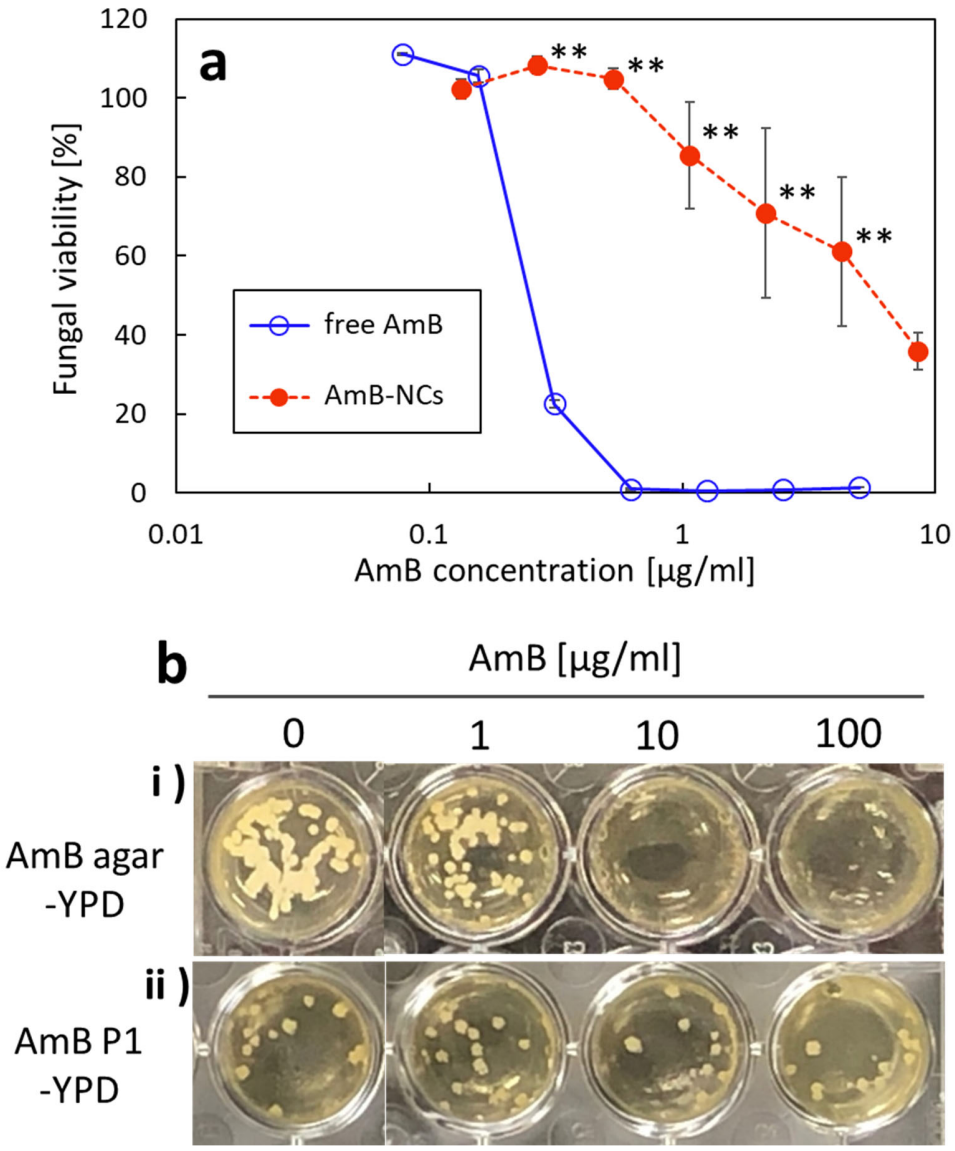

Figure 4. (a) Antifungal activity assay of AmB-NCs and free AmB using *Saccharomyces cerevisiae*. *S. cerevisiae* was cultured in a liquid YPD medium. (b) Antifungal activity of AmB toward *S. cerevisiae* cultured on gelated YPD media. (i) YPD medium containing AmB gelated with agar (AmB agar-YPD). (ii) YPD medium containing AmB gelated with P1 (AmB P1-YPD). *S. cerevisiae* was cultured for three days.

In our previous study, we prepared the co-assembly of a hydrophobic drug with P1 and succeeded in releasing the drug by degrading P1 with α-chymotrypsin (ChT).[32] In the present study, we also tried to release AmB from the AmB-NCs using ChT. The growth of *S. cerevisiae* was monitored over time in a liquid YPD medium (Fig. 5a). In the medium containing free AmB, the growth of *S. cerevisiae* was inhibited for a while and then rose after more than 20 h. In contrast, the growth in the medium containing AmB-NCs (1 μg mL^{-1}) started within a few hours, which was the same as the control (without additives). The induction times until the logarithmic growth phase started can be compared directly each other in a set of the culturing experiments at the same time. When *S. cerevisiae* was cultured in the medium containing 3.3 μg mL^{-1} ChT and 1 μg mL^{-1} AmB-NCs, the cell growth was delayed by approximately 7 h but was earlier than that of free AmB. The delay was caused by the degradation of P1 by ChT, i.e., degradation of P1 by ChT takes some time but leads to the release of AmB from the AmB-NCs into the medium. Figure 5b summarizes the antifungal activity (IC_{50}) of free AmB, AmB-NCs, and AmB-NCs with ChT. The IC_{50} values for free AmB, AmB-P1 NCs, and AmB-P1 NCs degraded by ChT were determined to be 0.25, 5.1, and 0.40 μg mL^{-1}, respectively. The antifungal activity of AmB was suppressed to approx. 1/20 by co-assembly with P1 and recovered to a value close to that of free AmB following degradation of P1 by ChT.

The release of AmB from hydrogels was examined. A phosphate buffer solution containing ChT was added on the AmB-P1 gel and the AmB-agar gel. AmB released to the liquid phase was periodically monitored using HPLC (Fig. 5c). In the absence of ChT, the release of AmB from the AmB-P1 gel was very low and a small amount of AmB continued to be released for at least 24 h. The AmB-agar gel released AmB faster than AmB-P1 gel. The amounts of AmB released from the AmB-agar gel and the AmB-P1 gel for 24 h were 23% and 3.8%, respectively. The difference

of releasing rate would be associated with the states of AmB molecules in the gels: AmB in the AmB-agar gel had a weak interaction with the agarose gel network and that in the AmB-P1 gel was bound to P1 via co-assembly. When ChT was added on the AmB-P1 gel, the release of AmB was remarkably accelerated. The release rate from the AmB-P1 gel with ChT was much faster than that of the AmB-agar gel. The enzymatic degradation of P1 in the AmB-P1 gel released free AmB, which led to the recovered antibacterial property observed in Fig. 5a & b.

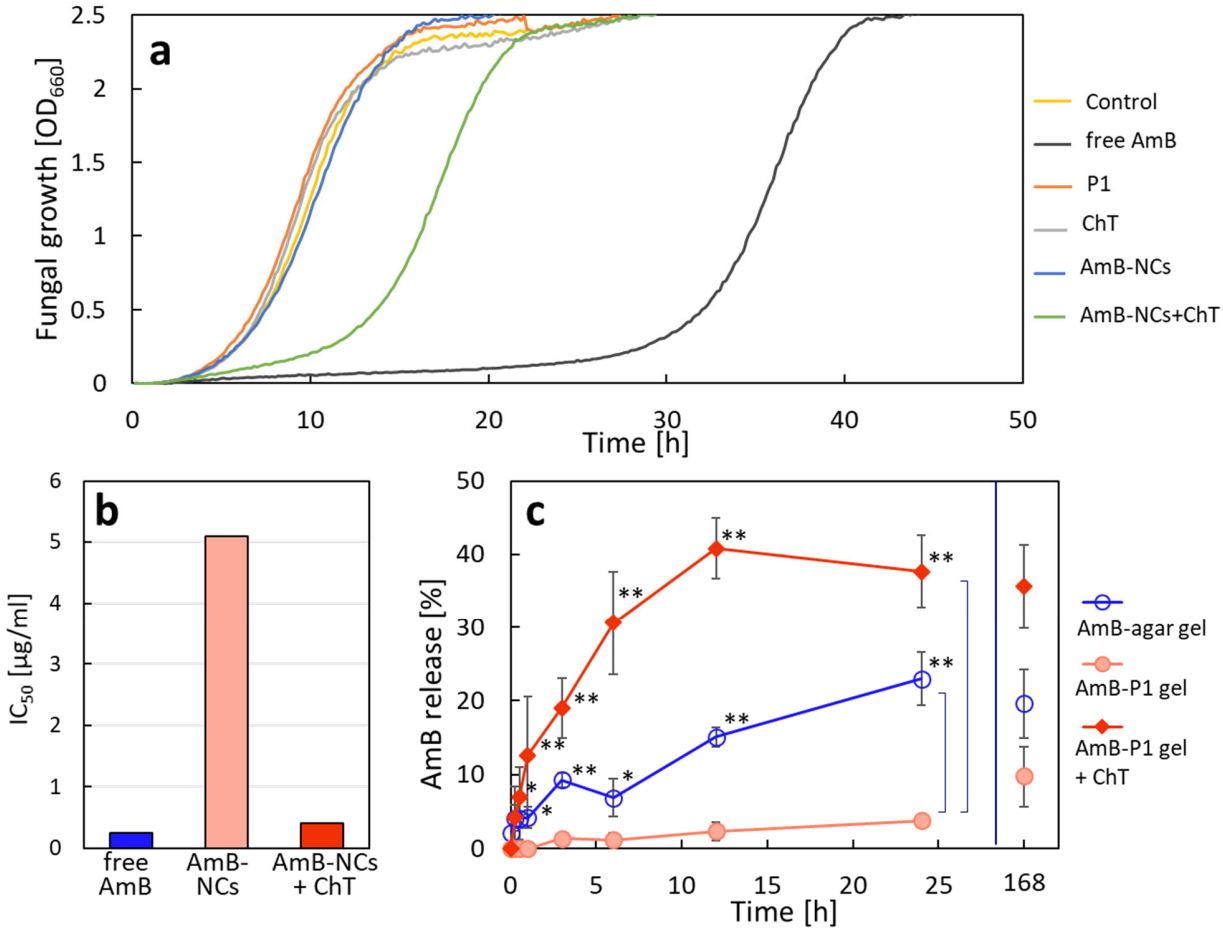

Figure 5. (a) Growth of *S. cerevisiae* in liquid YPD medium containing AmB or AmB-NCs. The AmB concentration was set at 1 μg mL^{-1}, except for the control. The P1 concentration was 0.2 wt%. ChT was used at 3.3 μg mL^{-1}. (b) Calculated IC_{50} values of AmB, the AmB-NCs, and the AmB-NCs with ChT for *S. cerevisiae.* (c) AmB-releasing profiles from hydrogels containing AmB.

A ChT solution (or a phosphate buffer solution) was added on hydrogels and the AmB concentration in the liquid phase was periodically monitored using HPLC.

We investigated the antifungal activity of the AmB-NCs to a fungus that secretes proteases. *A. oryzae* was used as a model fungus secreting proteases, and *S. cerevisiae* was used as a control fungus that does not secrete proteases. It was reported that *A. oryzae* secreted proteases in a modified Czapek-Dox medium (MCD medium).[38] The proteases cleaved protein at hydrophobic amino acids. We gelated MCD media with agar and P1. *A. oryzae* secreted proteases on the gelated MCD media (Fig. 6a). It was reported that the proteases cleaved peptide bonds at hydrophobic amino acids including phenylalanine.[38] After culturing, the MADI-TOF/MS analysis of the medium gelated with P1 revealed that P1 was degraded to several sort of peptide fragments (Fig. S6).

S. cerevisiae and *A. oryzae* were cultured on gelated MCD media containing 100 μg mL^{-1} AmB. Both *S. cerevisiae* and *A. oryzae* did not form any colonies on the MCD medium gelated with agar, indicating that 100 μg mL^{-1} AmB was sufficient to inhibit their growth (Fig. 6b(i), (ii)). On the MCD medium gelated with P1, *S. cerevisiae* formed colonies, indicating that the antifungal activity of AmB was suppressed by co-assembly with P1 (Fig. 6b(iii)). However, *A. oryzae* did not grow on the MCD medium gelated with P1. This observation indicated that proteases secreted from *A. oryzae* degraded P1 and released AmB from the gel (Fig. 6b(iv)). Indeed, when a YPD medium gelated by P1 was used for *A. oryzae* growth, *A. oryzae* grew on the medium because of negligible secretion of proteases (Fig. S7). These results demonstrated that the co-assembly of AmB with P1 endowed selective AmB activity.

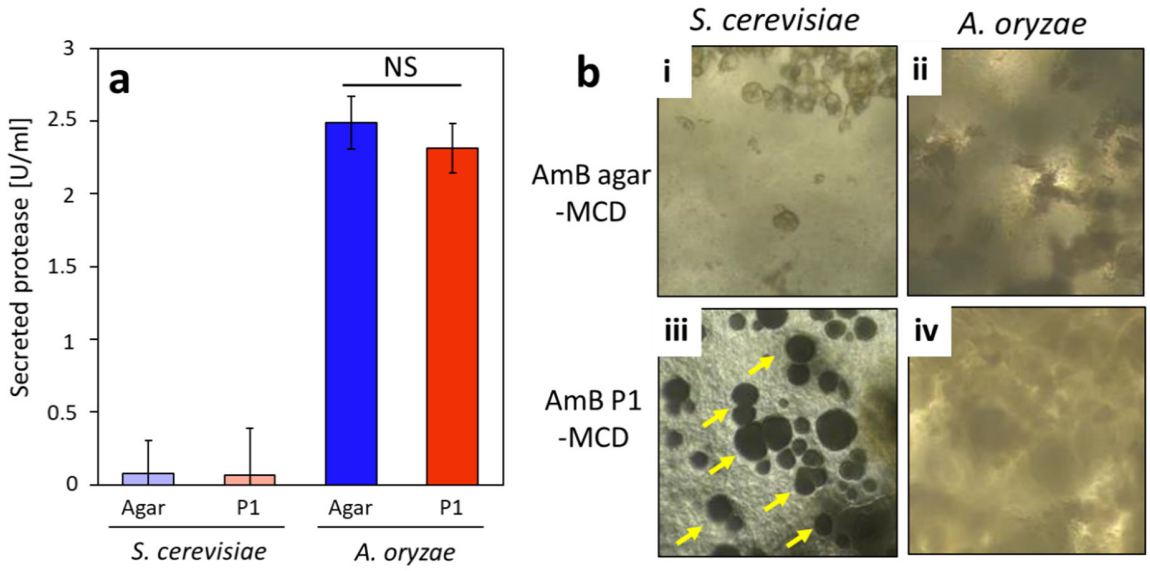

Figure 6. (a) Protease secretion from *S. cerevisiae* and *A. oryzae* cultured on modified Czapek-Dox (MCD) media gelated with agar and P1. (b) Antifungal activity assay of media containing 100 μg mL^{-1} AmB gelated with (i, ii) agar and (iii, iv) P1. (i, iii) *S. cerevisiae* and (ii, iv) *A. oryzae*. Image: 1 x 1 mm. Yellow arrows indicate colonies.

4. CONCLUSIONS

We successfully prepared the co-assembly of a short-peptide hydrogelator and a conventional antifungal drug. P1 and AmB were co-assembled into nanofibrous complexes whose length changed along the P1 concentration, which led to control the gelation properties of P1. The formation of the co-assembly masked the antifungal activity of AmB, and this activity was recovered by enzymatic degradation of this co-assembly. The co-assembly showed remarkable selective antifungal activity towards a fungus that secreted proteases but not towards a fungus that did not secrete proteases. Thus, this co-assembly should preserve indigenous fungi in humans. The present study proposed two different formulations for the antibacterial co-assembly: one was a gel

and the other is a dispersion solution. The gel formulation can be used as an ointment and the dispersion formulation can be used for administration by injection and inhalation.

Because of the challenges associated with developing new drugs, there is high demand to reposition conventional drugs to target other diseases. The combination of conventional drugs with assembling molecules should have significant potential to expand the application spectrum of conventional drugs via "drug repositioning."

ASSOCIATED CONTENT

Supporting Information: Materials, Experimental and Supplementary Results including MS data of P1, gelation properties of P1 with AmB, antibacterial activity assay of kanamycin with or without P1, inhibition of free AmB by P1 nano-assembly without heating, magnified SPM images, rheology measurements, protease-secretion and growth of fungi on gelated YPD media (DOCX).

AUTHOR INFORMATION

Corresponding Author

* tmarutcm@crystal.kobe-u.ac.jp

Funding Sources

This study was financially supported by JSPS KAKENHI Grant Numbers 19H05458 (T.M.), 20H02542 (T.M.), 21K18850 (T.M.), 20K22533 (K.M.), and 21K14471 (K.M.). This study was

partially supported by Takeda Science Foundation and Kawanishi Memorial ShinMaywa Education Foundation.

Notes

The authors declare no competing financial interest.

ACKNOWLEDGMENT

We thank Prof. Matsuyama (Kobe Univ) and Prof. Matsuoka (Kobe Univ) for technical help in rheology measurements. We thank Edanz (https://jp.edanz.com/ac) for editing a draft of this manuscript.

REFERENCES

(1) Durand, G. A.; Raoult, D.; Dubourg, G. Antibiotic Discovery: History, Methods and Perspectives. *Int. J. Antimicrob. Agents* **2019**, *53* (4), 371–382. https://doi.org/10.1016/j.ijantimicag.2018.11.010.

(2) Hutchings, M.; Truman, A.; Wilkinson, B. Antibiotics: Past, Present and Future. *Curr. Opin. Microbiol.* **2019**, *51*, 72–80. https://doi.org/10.1016/j.mib.2019.10.008.

(3) Aminov, R. I. A Brief History of the Antibiotic Era: Lessons Learned and Challenges for the Future. *Front. Microbiol.* **2010**, *1* (134), 1–7. https://doi.org/10.3389/fmicb.2010.00134.

(4) Dheman, N.; Mahoney, N.; Cox, E. M.; Farley, J. J.; Amini, T.; Lanthier, M. L. An Analysis of Antibacterial Drug Development Trends in the United States, 1980–2019. *Clin. Infect. Dis.* **2021**, *73* (11), E4444–E4450. https://doi.org/10.1093/cid/ciaa859.

(5) Brown, E. D.; Wright, G. D. Antibacterial Drug Discovery in the Resistance Era. *Nature* **2016**, *529* (7586), 336–343. https://doi.org/10.1038/nature17042.

(6) Zhu, P.; Cai, L.; Liu, Q.; Feng, S.; Ruan, H.; Zhang, L.; Zhou, L.; Jiang, H.; Wang, H.; Wang, J.; Chen, J. One-Pot Synthesis of α-Linolenic Acid Nanoemulsion-Templated Drug-Loaded Silica Mesocomposites as Efficient Bactericide against Drug-Resistant Mycobacterium Tuberculosis. *Eur. J. Pharm. Sci.* **2022**, *176* (May), 106261. https://doi.org/10.1016/j.ejps.2022.106261.

(7) Ashburn, T. T.; Thor, K. B. Drug Repositioning: Identifying and Developing New Uses for Existing Drugs. *Nat. Rev. Drug Discov.* **2004**, *3* (8), 673–683. https://doi.org/10.1038/nrd1468.

(8) Kumar, R.; Harilal, S.; Gupta, S. V.; Jose, J.; Thomas, D. G.; Uddin, M. S.; Shah, M. A.; Mathew, B. Exploring the New Horizons of Drug Repurposing: A Vital Tool for Turning Hard Work into Smart Work. *Eur. J. Med. Chem.* **2019**, *182*, 111602. https://doi.org/10.1016/j.ejmech.2019.111602.

(9) Wu, C.; Liu, Y.; Yang, Y.; Zhang, P.; Zhong, W.; Wang, Y.; Wang, Q.; Xu, Y.; Li, M.; Li, X.; Zheng, M.; Chen, L.; Li, H. Analysis of Therapeutic Targets for SARS-CoV-2 and Discovery of Potential Drugs by Computational Methods. *Acta Pharm. Sin. B* **2020**, *10* (5), 766–788. https://doi.org/10.1016/j.apsb.2020.02.008.

(10) Messer, S. A.; Moet, G. J.; Kirby, J. T.; Jones, R. N. Activity of Contemporary Antifungal Agents, Including the Novel Echinocandin Anidulafungin, Tested against Candida Spp., Cryptococcus Spp., and Aspergillus Spp.: Report from the SENTRY Antimicrobial Surveillance Program (2006 to 2007). *J. Clin. Microbiol.* **2009**, *47* (6), 1942–1946. https://doi.org/10.1128/JCM.02434-08.

(11) Tortorano, A. M.; Prigitano, A.; Morroni, G.; Brescini, L.; Barchiesi, F. Candidemia: Evolution of Drug Resistance and Novel Therapeutic Approaches. *Infect. Drug Resist.* **2021**, *14*, 5543–5553. https://doi.org/10.2147/idr.s274872.

(12) Ellis, D. Amphotericin B: Spectrum and Resistance. *J. Antimicrob. Chemother.* **2002**, *49* (SUPL. S1), 7–10. https://doi.org/10.1093/jac/49.suppl_1.7.

(13) Laniado-Laborín, R.; Cabrales-Vargas, M. N. Amphotericin B: Side Effects and Toxicity. *Rev. Iberoam. Micol.* **2009**, *26* (4), 223–227. https://doi.org/10.1016/j.riam.2009.06.003.

(14) Eriksson, U.; Seifert, B.; Schaffner, A. Comparison of Effects of Amphotericin B Deoxycholate Infused over 4 or 24 Hours: Randomised Controlled Trial. *Br. Med. J.* **2001**, *322* (7286), 579–582. https://doi.org/10.1136/bmj.322.7286.579.

(15) Kamiński, D. M. Recent Progress in the Study of the Interactions of Amphotericin B with Cholesterol and Ergosterol in Lipid Environments. *Eur. Biophys. J.* **2014**, *43* (10–11), 453–467. https://doi.org/10.1007/s00249-014-0983-8.

(16) Matsumori, N.; Tahara, K.; Yamamoto, H.; Morooka, A.; Doi, M.; Oishi, T.; Murata, M. Direct Interaction between Amphotericin B and Ergosterol in Lipid Bilayers as Revealed by 2H NMR Spectroscopy. *J. Am. Chem. Soc.* **2009**, *131* (33), 11855–11860. https://doi.org/10.1021/ja9033473.

(17) Saka, Y.; Mita, T. Interaction of Amphotericin B with Cholesterol in Monolayers, Aqueous Solutions, and Phospholipid Bilayers. *J. Biochem.* **1998**, *123* (5), 798–805. https://doi.org/10.1093/oxfordjournals.jbchem.a022007.

(18) Latgé, J. P. Aspergillus Fumigatus and Aspergillosis. *Clin. Microbiol. Rev.* **1999**, *12* (2), 310–350. https://doi.org/10.1128/cmr.12.2.310.

(19) Abad-zapatero, C.; Goldman, R.; Muchmore, S. W.; Hutchins, C.; Stewart, K.; Navaza, J.; Payne, C. D.; Ray, T. L.; Group, A.; Laboratories, A.; Park, A. Structure of a Secreted Aspartic Protease from C. Albicans Complexed with a Potent Inhibitor: Implications for the Design of Antifungal Agents. *Protein Sci.* **1996**, *5*, 640–652.

(20) Kryštůfek, R.; Šácha, P.; Starková, J.; Brynda, J.; Hradilek, M.; Tloušťová, E.; Grzymska, J.; Rut, W.; Boucher, M. J.; Drąg, M.; Majer, P.; Hájek, M.; Řezáčová, P.; Madhani, H. D.; Craik, C. S.; Konvalinka, J. Re-Emerging Aspartic Protease Targets: Examining Cryptococcus Neoformans Major Aspartyl Peptidase 1 as a Target for Antifungal Drug Discovery. *J. Med. Chem.* **2021**, *64* (10), 6706–6719. https://doi.org/10.1021/acs.jmedchem.0c02177.

(21) Martinez, D. A.; Oliver, B. G.; Gräser, Y.; Goldberg, J. M.; Li, W.; Martinez-Rossi, N. M.; Monod, M.; Shelest, E.; Barton, R. C.; Birch, E.; Brakhage, A. A.; Chen, Z.; Gurr, S. J.; Heiman, D.; Heitman, J.; Kosti, I.; Rossi, A.; Saif, S.; Samalova, M.; Saunders, C. W.; Shea, T.; Summerbell, R. C.; Xu, J.; Young, S.; Zeng, Q.; Birren, B. W.; Cuomo, C. A.; White, T. C. Comparative Genome Analysis of Trichophyton Rubrum and Related Dermatophytes Reveals Candidate Genes Involved in Infection. *MBio* **2012**, *3* (5). https://doi.org/10.1128/mBio.00259-12.

(22) Monod, M.; Capoccia, S.; Léchenne, B.; Zaugg, C.; Holdom, M.; Jousson, O. Secreted Proteases from Pathogenic Fungi. *Int. J. Med. Microbiol.* **2002**, *292* (5–6), 405–419. https://doi.org/10.1078/1438-4221-00223.

(23) Gräser, Y.; Monod, M.; Bouchara, J. P.; Dukik, K.; Nenoff, P.; Kargl, A.; Kupsch, C.; Zhan, P.; Packeu, A.; Chaturvedi, V.; De Hoog, S. New Insights in Dermatophyte Research. *Med. Mycol.* **2018**, *56*, S2–S9. https://doi.org/10.1093/mmy/myx141.

(24) Maeda, H. Role of Microbial Proteases in Pathogenesis. *Microbiol. Immunol.* **1996**, *40* (10), 685–699. https://doi.org/10.1111/j.1348-0421.1996.tb01129.x.

(25) Du, X.; Zhou, J.; Shi, J.; Xu, B. Supramolecular Hydrogelators and Hydrogels: From Soft Matter to Molecular Biomaterials. *Chem. Rev.* **2015**, *115* (24), 13165–13307. https://doi.org/10.1021/acs.chemrev.5b00299.

(26) Suzuki, M.; Yumoto, M.; Shirai, H.; Hanabusa, K. Supramolecular Gels Formed by Amphiphilic Low-Molecular-Weight Gelators of Nα-Nεdiacyl-L-Lysine Derivatives. *Chem. - A Eur. J.* **2008**, *14* (7), 2133–2144. https://doi.org/10.1002/chem.200701111.

(27) De Loos, M.; Feringa, B. L.; Van Esch, J. H. Design and Application of Self-Assembled Low Molecular Weight Hydrogels. *European J. Org. Chem.* **2005**, No. 17, 3615–3631. https://doi.org/10.1002/ejoc.200400723.

(28) Bieser, A. M.; Tiller, J. C. Structure and Properties of Low Molecular Weight Hydrogelators. *J. Phys. Chem. B* **2007**, *111*, 13180–13187. https://doi.org/10.1021/jp076495x.

(29) Tanaka, A.; Fukuoka, Y.; Morimoto, Y.; Honjo, T.; Koda, D.; Goto, M.; Maruyama, T. Cancer Cell Death Induced by the Intracellular Self-Assembly of an Enzyme-Responsive Supramolecular Gelator. *J. Am. Chem. Soc.* **2015**, *137* (2), 770–775. https://doi.org/10.1021/ja510156v.

(30) Restu, W. K.; Yamamoto, S.; Nishida, Y.; Ienaga, H.; Aoi, T.; Maruyama, T. Hydrogel Formation by Short D-Peptide for Cell-Culture Scaffolds. *Mater. Sci. Eng. C* **2020**, *111*, 110746. https://doi.org/10.1016/j.msec.2020.110746.

(31) Yamamoto, S.; Nishimura, K.; Morita, K.; Kanemitsu, S.; Nishida, Y.; Morimoto, T.; Aoi, T.; Tamura, A.; Maruyama, T. Microenvironment PH-Induced Selective Cell Death for

Potential Cancer Therapy Using Nanofibrous Self-Assembly of a Peptide Amphiphile. *Biomacromolecules* **2021**, *22* (6), 2524–2531. https://doi.org/10.1021/acs.biomac.1c00267.

(32) Restu, W. K.; Nishida, Y.; Yamamoto, S.; Ishii, J.; Maruyama, T. Short Oligopeptides for Biocompatible and Biodegradable Supramolecular Hydrogels. *Langmuir* **2018**, *34* (27), 8065–8074. https://doi.org/10.1021/acs.langmuir.8b00362.

(33) Albadr, A. A.; Coulter, S. M.; Porter, S. L.; Thakur, R. R. S.; Laverty, G. Ultrashort Self-Assembling Peptide Hydrogel for the Treatment of Fungal Infections. *Gels* **2018**, *4* (2), 1–15. https://doi.org/10.3390/gels4020048.

(34) Fleming, S.; Ulijn, R. V. Design of Nanostructures Based on Aromatic Peptide Amphiphiles. *Chem. Soc. Rev.* **2014**, *43* (23), 8150–8177. https://doi.org/10.1039/c4cs00247d.

(35) Panja, S.; Dietrich, B.; Adams, D. J. Controlling Syneresis of Hydrogels Using Organic Salts. *Angew. Chemie - Int. Ed.* **2022**, *61* (4), 1–6. https://doi.org/10.1002/anie.202115021.

(36) Basu, K.; Baral, A.; Basak, S.; Dehsorkhi, A.; Nanda, J.; Bhunia, D.; Ghosh, S.; Castelletto, V.; Hamley, I. W.; Banerjee, A. Peptide Based Hydrogels for Cancer Drug Release: Modulation of Stiffness, Drug Release and Proteolytic Stability of Hydrogels by Incorporating d-Amino Acid Residue(S). *Chem. Commun.* **2016**, *52* (28), 5045–5048. https://doi.org/10.1039/c6cc01744d.

(37) Skilling, K. J.; Citossi, F.; Bradshaw, T. D.; Ashford, M.; Kellam, B.; Marlow, M. Insights into Low Molecular Mass Organic Gelators: A Focus on Drug Delivery and Tissue Engineering Applications. *Soft Matter* **2014**, *10* (2), 237–256. https://doi.org/10.1039/c3sm52244j.

(38) Kumura, H.; Ishido, T.; Shimazaki, K. Production and Partial Purification of Proteases from Aspergillus Oryzae Grown in a Medium Based on Whey Protein as an Exclusive Nitrogen Source. *J. Dairy Sci.* **2011**, *94* (2), 657–667. https://doi.org/10.3168/jds.2010-3587.

(39) Ojima, Y.; Sawabe, T.; Konami, K.; Azuma, M. Construction of Hypervesiculation Escherichia Coli Strains and Application for Secretory Protein Production. *Biotechnol. Bioeng.* **2020**, *117* (3), 701–709. https://doi.org/10.1002/bit.27239.

(40) Shiina, S.; Ohshima, T.; Sato, M. Extracellular Release of Recombinant α-Amylase from Escherichia Coli Using Pulsed Electric Field. *Biotechnol. Prog.* **2004**, *20* (5), 1528–1533. https://doi.org/10.1021/bp049760u.

TABLE OF CONTENTS

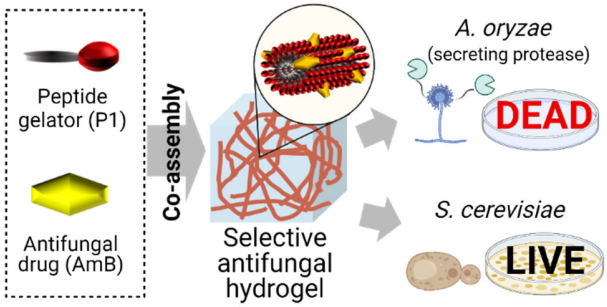

Novel antifungal selectivity was created in a conventional antifungal drug, amphotericin B (AmB) via the co-assembly formation with a short-peptide hydrogelator (P1). The co-assembly complex suppressed the intrinsic antifungal activity. When P1 in the complex was degraded by a protease secreted from a fungus, the suppressed antifungal activity of AmB recovered, resulting in the selective killing of the fungus.